Optically pumped generation of multi-pulse three-wave coupled states in a two-mode waveguide with a square-law nonlinearity and digital modulation of light

A.S. Shcherbakov
National Institute for Astrophysics, Optics & Electronics,
Apartado Postal 51 y 216, Puebla, 72000, Mexico,
Phone: 52 (222) 266 3100, ext. 2205; Fax: 52 (222) 247 2940,
e-mail: alex@inaoep.mx

A. Aguirre Lopez
Mixteca University of Technology,
Huajuapan de Leon, Oaxaca, 69000, Mexico,
Phone: 52 (953) 532 0399, ext. 500; Fax: 52 (953) 532 0214,
e-mail: aaguirre@mixteco.utm.mx

Recibido el 2 de octubre de 2007; aceptado el 11 de septiembre de 2008

We study the process of sculpturing three-wave weakly coupled states under the action of the pulsed optical pump in a two-mode square-law nonlinear waveguide within the collinear regime of propagating the interacting waves. The analytical model for this process with slightly mismatched wave numbers predicts the sculpturing of multi-pulse optical components inherent in three-wave coupled states. Reasoning from the developed approach, we discuss an opportunity for the digital modulation of light, because those potentially three-wave coupled states under consideration can be binary encoded. The performed analysis of sculpturing multi-pulse coupled states in a non-stationary regime was experimentally examined during our studies of collinear acousto-optical interaction in a two-mode lithium niobate waveguiding structure exhibiting a square-law nonlinearity.

Keywords: Three-wave collinear interaction; optical pump; multi-pulse three-wave coupled states; square-law nonlinearity.

Se estudió el proceso para obtener tres estados débilmente ligados por bombeo óptico pulsado en una guía de ondas no lineal de variación cuadrática doble dentro del régimen colineal de propagación de ondas interactuantes. El modelo analítico para este proceso con números de onda en ligera discordancia predice este fenómeno. En base a lo anterior se discute la modulación digital de la luz debida a que, potencialmente, los tres estados acoplados bajo estudio pueden ser codificaos en forma binaria. Se realizó el análisis experimental del fenómeno anterior a través del estudio de la interacción acustóptica colineal en una guía de ondas de niobato del litio y se observó un comportamiento cuadrático.

Descriptores: Interacción coolineal de tres ondas; bombeo óptico; estados acoplados de tres ondas; ley cuadrática.

PACS: 32.80.Xx;

1. Introduction

In the last few years, the investigations of wave processes in square-law nonlinear media had led to the discovery of various solitary waves in the form of multi-wave coupled states, whose components of even different physical nature are mutually trapped and propagate together [1-3]. The profiles of all the interacting waves are steady at three different current frequencies, because the interaction exhibits itself as a mechanism of the stabilizing self-action [4]. Mismatching the wave numbers can be also included in a similar analysis that gives us the opportunity to follow the process more sequentially [5]. The three-wave coupled states represent, clearly, the simplest version of multi-wave solitary waves in a square-law nonlinear medium due to the balancing action of this type of nonlinearity. By this is meant, in particular, that three-wave coupled states can be shaped via, for example, three-wave acousto-optical interaction in a weakly anisotropic medium. Recently, similar solitary waves have been described, observed, and studied due to our previous research into this phenomenon in both the collinear and non-collinear regimes of propagating the interacting waves with the continuous-wave incident light wave as a pump [6,7]. By contrast, the main aspect of this work is connected with the shaping of three-wave weakly coupled states under the pumping action of the incoming optical pulses. In so doing, we present the results of studying three-wave weakly coupled states in the particular case of co-directional collinear light scattering by a relatively slow non-optical wave. The presented non-stationary model offers a clear view of this phenomenon with the mismatched wave numbers and predicts the sculpturing of multi-pulse three-wave weakly coupled states. The development of weakly coupled states is possible only when the generating non-optical wave and the incident light beam are present simultaneously in the same interaction area, and each of them can be equally well taken as the parameter that controls the interaction. This fact allows us to use this effect to shape weakly coupled states by the incom-

ing pulses, *i.e.* by the pump for controlling the data stream associated with the incoming optical pulse train that can be binary encoded. In this case, control will be provided by an electronic digital signal, presented in a medium by a binary encoded sequence of non-optical pulses. The analysis was examined experimentally using the collinear acousto-optical interaction in a two-mode square-law nonlinear waveguide.

In Sec. 2, the mathematical model for describing the collinear three-wave interaction in a square-law, nonlinear, weakly anisotropic medium is presented. Here, we discuss some natural restrictions simplifying the set of evolution equations, and illustrate the properties of the developed model. Then, the regime of weakly coupled states in a two-mode waveguide as well as the localization conditions in non-stationary regime are described in Sec. 3, where the stages of passing a rectangular in shape non-optical pulse are sequentially followed. The possibilities for shaping various multi-pulse trains of three-wave weakly coupled states by optical pump and realizing the digital modulation of light based on exploiting collinear three-wave coupled states are considered in Sec. 4. Together with this in Sec. 5, we select and describe the physical mechanism that is acceptable for the adequate experimental application of the model developed. The needed estimations and some details of experimental procedure, including general and optical schemes as well as the oscilloscope traces obtained, are touched on Sec. 6. Section 7 presents our concluding remarks regarding both theoretical and experimental aspects of the work presented.

2. Mathematical model for describing a three-wave collinear interaction in a square-law nonlinear weakly anisotropic medium

Originally, the co-directional collinear interaction for a triplet of waves in a square-law nonlinear weakly anisotropic medium is described by the following set of partial differential equations [5,8]:

$$\frac{\partial C_0}{\partial x}+\frac{1}{c_0}\frac{\partial C_0}{\partial t}=q_1 C_1 U\exp\left(-2\,i\,\eta\,x\right),$$
$$\frac{\partial C_1}{\partial x}+\frac{1}{c_1}\frac{\partial C_1}{\partial t}=-q_0 C_0 U^*\exp\left(2\,i\,\eta\,x\right),$$
$$\frac{\partial U}{\partial x}+\frac{1}{v}\frac{\partial U}{\partial t}=-q_U C_0 C_1^*\exp\left(2\,i\,\eta\,x\right). \qquad (1)$$

In the context of the problem under consideration, C_0, C_1, U and c_0, c_1, v represent the complex amplitudes and group velocities of two optical waves and one non-optical one, respectively; q_0, q_1, q_U are the interaction factors; $2\eta = k_1 - k_0 - k_U$ is the mismatch between the wave numbers k_0, k_1, and k_U belonging to the corresponding waves. The wave number k_U of the non-optical wave can be presented as $k_U = k + \Delta k$, where k is the wave number corresponding to the regime of exact phase synchronism, while $\Delta k = 2\pi\Delta f/v$ reflects the deviation from that synchronism due to a variation Δf of the current cyclic frequency f inherent in the non-optical wave. Often, the values of $k_0 = 2\pi n_0/\lambda$ and $k_0 = 2\pi n_1/\lambda$ are fixed for the chosen initial light wavelength λ in a waveguide with the refractive indices n_0 and n_1, so that $k_1 - k_0 - k = 0$. Consequently, one can write $\eta = \pi\Delta f/v$ and hence $\eta = 0$ with $\Delta f = 0$ in the regime of exact phase synchronism. The inequality $v < c_1 < c_0$ between the group velocities and the signs presented on the right hand side of Eqs.(1) are related to a regime of the decay instability when the energy exchange takes place between all the interacting waves.

Usually, the difference $|n_0 - n_1|$ between the refractive indices in optically transparent materials is too small, so that sometimes it seems reasonable to approximate the velocities of light modes as $c_0/c_1 \approx 1$. To determine an area of applicability for such an approximation let us consider the interaction between two optical pulses of width T_0 in a weakly anisotropic medium. If initially these two pulses are spatially overlapping, they will be separated from each other at the distance $L_0 \approx c_{0,1}T_0\left(1 - c_1/c_0\right)^{-1}$. Thus, the distance L_0 characterizes the length of the collinear three-wave interaction in the chosen approximation. For typical widths of non-optical pulses exceeding $1ns$ and for the anisotropy of about $(1 - c_1/c_0) \leq 0.1$, one can obtain the following estimate: L_0 >100m. Such a length of interaction is unattainable in crystalline optical waveguides, because usually the waveguide length does not exceed 10cm, so that one can approximate the velocities of light modes as $c_0 \approx c_1 \approx c$ in Eqs.(1).

Here, we consider a regime of weak coupling, when two light modes are connected with each other via an additional pulse of a relatively slow wave, being non-optical in nature nevertheless, an essentially effective interaction between light modes can be achieved without any observable influence of the interaction process on that non-optical wave, because the number of interacting photons is a few orders less than the number of scattering non-optical quanta injected into a waveguide. In this case, the set of equations (1) falls into a homogeneous wave equation for a slow non-optical wave, which possesses the traveling-wave solution $U = U\left(x - vt\right)$, and a pair of the combined equations for light wave amplitudes. The complex amplitudes $C_0\left(x,t\right)$ and $C_1\left(x,t\right)$, describing the pumping light mode and generated one respectively, are governed by

$$\frac{\partial C_0}{\partial x}+\frac{1}{c}\frac{\partial C_0}{\partial t}=-q_1 C_1 U^*\left(x-vt\right)\exp\left(2\,i\,\eta\,x\right), \qquad (2)$$
$$\frac{\partial C_1}{\partial x}+\frac{1}{c}\frac{\partial C_1}{\partial t}=q_0 C_0 U^*\left(x-vt\right)\exp\left(-2\,i\,\eta\,x\right). \qquad (3)$$

A pair of Eqs.(2) and (3) allows the following simple transformations. First, Eq.(2) can be multiplied by C_0^*; second, the complex conjugate of the obtained result can be written as well. Summarizing these two expressions, one can calculate

$$\frac{\partial\left|C_0\right|^2}{\partial x}+\frac{1}{c}\frac{\partial\left|C_0\right|^2}{\partial t}=-q_1 C_0^* C_1 U^*\left(x-vt\right)\exp\left(2\,i\,\eta\,x\right)$$
$$-\,q_1 C_0 C_1^* U^*\left(x-vt\right)\exp\left(-2\,i\,\eta\,x\right). \qquad (4)$$

Similar calculations can be performed for Eq.(3) using C_1^*, so that the result is given by

$$\frac{\partial |C_1|^2}{\partial x} + \frac{1}{c}\frac{\partial |C_1|^2}{\partial t} = q_0 C_0^* C_1 U^*(x - vt)\exp(2\,i\,\eta\,x) + q_0 C_0 C_1^* U^*(x - vt)\exp(-2\,i\,\eta\,x). \quad (5)$$

Multiplying Eq.(4) by q_0, Eq.(5) by q_1 and summarizing these results, one can obtain

$$\left(\frac{\partial}{\partial x} + \frac{1}{c}\frac{\partial}{\partial t}\right)\left(q_0 |C_0|^2 + q_1 |C_1|^2\right) = 0. \quad (6)$$

Finally, exploiting the boundary conditions $C_0(x = 0, t) = 1$ and $C_1(x = 0, t) = 0$ that are natural for Eqs.(2) and (3), we arrive at the following conservation law:

$$q_0 |C_0|^2 + q_1 |C_1|^2 = q_0. \quad (7)$$

Now, we go to the tracking coordinate system $(z = x, \tau = t - x/c)$. Because $t = \tau + z/c$ in this case, one can obtain that $U(x - vt) = U[z(1 - v/c) - v\tau]$ and

$$\frac{\partial C_{0,1}}{\partial x} + \frac{1}{c}\frac{\partial C_{0,1}}{\partial t} = \frac{\partial C_{0,1}}{\partial z}.$$

Making the back substitutions in Eqs.(2) and (3), we arrive at

$$\frac{\partial C_0}{\partial x} = -q_1 C_1 U^*\left[x\left(1 - \frac{v}{c}\right) - v\tau\right]\exp(2\,i\,\eta\,x), \quad (8)$$

$$\frac{\partial C_1}{\partial x} = -q_0 C_0 U^*\left[x\left(1 - \frac{v}{c}\right) - v\tau\right]\exp(-2\,i\,\eta\,x) \quad (9)$$

These equations represent the simplified model of the problem under consideration. To illustrate the properties of these models let us consider the particular case of $\eta = 0$, when the solutions to Eqs.(8), (9) with the boundary conditions $C_0(\tau, 0) = A_0$, and $C_1(\tau, 0) = 0$ an arbitrary shape of $U(x, \tau)$ may be written as

$$|C_0| = A_0\cos\varphi; \quad |C_1| = A_0\sqrt{\frac{q_0}{q_1}}\sin\varphi$$

$$\varphi(x, t) = \beta\int_0^x |U(x, \tau)|\,dx; \quad \beta = \sqrt{q_0 q_1}. \quad (10)$$

As follows from Eqs.(10), when $\varphi = \pi N$ (here N is the whole number), the amplitude of the generated light wave is equal to zero outside the non-optical wave pulse, so localization of the generated light occurs only inside the spatial interval occupied by the non-optical wave pulse. As this takes place, the spatial distribution of the generated light intensity contains N peaks of partial pulses, and simultaneously the distribution of the incident light has N holes at the same temporal positions. To demonstrate this phenomenon we consider an example in the coordinate system associated with the moving non-optical pulse, *i.e.* with $v = 0$, and take the non-optical wave pulse in the form of $|U(x)| = U_0\,\mathrm{sec\,h}(x/x_s)$ (here x_s is the spatial pulse width, its temporal width, *i.e.* its duration can be defined as $\tau_s = x_s v^{-1}$ at the level of $\mathrm{sec\,h}1 \approx 0.65$), whose envelope has infinite wings. We obtain from Eqs.(10) that

$$|C_0| = \cos\{\beta U_0 x_s \arctan[\sinh(x/x_s)]\},$$

$$|C_1| = \sin\{\beta U_0 x_s \arctan[\sinh(x/x_s)]\}. \quad (11)$$

Using Eqs.(11), the condition of localization can be written as $\beta U_0 x_s = N$. Thus, when $N = (1, 3, 5, \ldots)$, the wave C_0 forms an N-pulse bright component, while the wave C_1 manifests an N-pulse dark component (or shock wave), and conversely if $N = (2, 4, 6, ...)$, an N-pulse dark component appears in wave C_0 and an N-pulse bright component arises in wave C_1 each belongs to the corresponding multi-pulse coupled state. Figure 1 gives art illustrations for these relations when $N = 1, 2$ and $\beta = 2/\pi$. Figure 1a displays the localization with $N = 1$, $U_0 = 1$, and $x_p = \pi/2$, when a one-pulse coupled state is formed. The localization with $N = 2$ is done in two different ways, namely, with $U_0 = 1$ and $x_s = \pi$ (see Fig.1b) or with $U_0 = 2$ and $x_s = \pi/2$ (see Fig.1c). The last pair of diagrams reproduces two different kinds of two-pulse coupled states.

3. Three-wave weakly coupled states in a two-mode waveguide; the localization conditions in a non-stationary regime

Now we assume that non-optical pulse $U[x(1 - v/c) - v\tau] = u[x(1 - v/c) - v\tau]\exp(i\varphi)$ has the constant phase φ, and Eq.(8) and (9) can be converted into a pair of the complex-valued equations

$$\frac{\partial^2 C_{0,1}}{\partial x^2} - \left(\frac{1}{u}\frac{\partial u}{\partial x} \pm 2i\eta\right)\frac{\partial C_{0,1}}{\partial x} + q_0 q_1 u^2 C_{0,1} = 0. \quad (12)$$

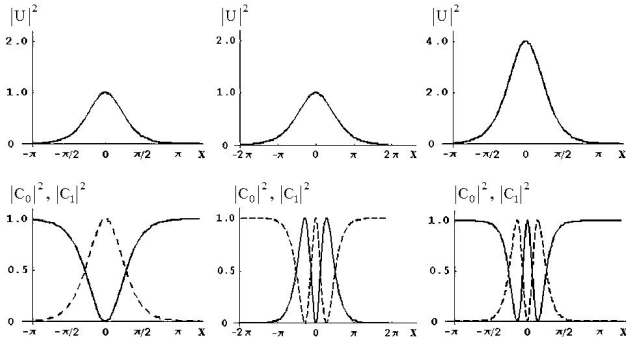

FIGURE 1. Spatial distributions for the components of coupled states versus the normalized coordinate x for $\beta = 2/\pi$: (a) localizing a one-pulse coupled state with $N = 1$, $U_0 = 1$, and $x_p = \pi/2$; (b) localizing a two-pulse coupled state with $N = 2$, $U_0 = 1$ and $x_s = \pi$; and (c) localizing a two-pulse coupled state with $N = 2$, $U_0 = 2$ and $x_s = \pi/2$. The upper diagrams illustrate the variations of $|U|^2$, the bottom diagrams show $|C_0|^2$ (dashed lines) and $|C_1|^2$ (solid lines).

We set $C_{0,1} = a_{0,1}(x,t)\exp[i\Phi_{0,1}(x,t)]$, $\gamma_{0,1} = \partial\Phi_{0,1}/\partial x$ and divide real and imaginary parts in Eq.(12) as

$$\frac{\partial^2 a_{0,1}}{\partial x^2} - \left(\frac{1}{u}\frac{\partial u}{\partial x}\right)\frac{\partial a_{0,1}}{\partial x} + \left(q_0 q_1 u^2 - \gamma_{0,1}^2 \pm 2\eta\gamma_{0,1}\right) a_{0,1} = 0, \quad (13)$$

$$2\left(\gamma_{0,1} \mp \eta\right)\frac{\partial a_{0,1}}{\partial x} + \left(\frac{\partial \gamma_{0,1}}{\partial x} - \frac{\gamma_{0,1}}{u}\frac{\partial u}{\partial x}\right) a_{0,1} = 0. \quad (14)$$

It follows from Eq.(14) that

$$\gamma_{0,1} = \pm\eta u a_{0,1}^{-2}\int u^{-1}\left(\partial a_{0,1}^2/\partial x\right)dx + \Gamma_{0,1} u a_{0,1}^{-2},$$

where $\Gamma_{0,1}$ are the integration constants. Now, we focus on the process of localization in the case, when first, two facets of a waveguide at $x = 0$ and $x = L$ restrict the area of interaction and the spatial length x_0 of the non-optical pulse is much less than L, and second, the non-optical pulse is represented by

$$u(x,t) = U_0\{\theta[x(1-v/c) - v\tau] - \theta[(x-x_0)(1-v/c) - v\tau]\},$$

i.e. it has a rectangular shape with amplitude U_0. We analyze Eqs.(13) and (14) with the fixed magnitude of η and rather natural boundary conditions $a_0(x=0,\tau) = 1$, $a_1(x=0,\tau) = 0$ and trace dynamics of the phenomenon With the assumption that $v \ll c$, we may put that $\partial U/\partial x \approx 0$ in Eqs.(13) and (14) everywhere, excluding the points $x \in \{0, x_0\}$, and obtain $\gamma_{0,1} = \pm\eta + \Gamma_{0,1}U_0 a_{0,1}^{-2}$. Then, we follow three stages inherent in the localization process.

Stage 1: The localizing pulse is incoming through the facet

$x = 0$. Exploiting the obtained values of $\gamma_{0,1}$, Eq.(13) can be solved exactly. The light wave intensities on $x \in \{0, x_0\}$ with $\Gamma_0 = \eta/U_0$, $\Gamma_1 = 0$, and $q_0 q_1 U_0^2 = \sigma^2$ are given by

$$|C_0|^2 = \frac{\eta^2}{\sigma^2+\eta^2} + \frac{\sigma^2}{\sigma^2+\eta^2}\cos^2\left(x\sqrt{\sigma^2+\eta^2}\right), \quad (15)$$

$$|C_1|^2 = \frac{q_0}{q_1}\frac{\sigma^2}{\sigma^2+\eta^2}\sin^2\left(x\sqrt{\sigma^2+\eta^2}\right). \quad (16)$$

To find the coefficients in Eqs.(15) and (16) we have used the conservation law $q_0 a_0^2 + q_1 a_1^2 = q_0$ [see Eq.(7)]. It can be seen from Eqs.(15) and (16) that, on the one hand, the efficiency of light scattering is going to 100% when $\eta \to 0$. On the other hand, when $\sigma^2 \ll \eta^2$, one can nevertheless observe the dynamics of shaping three-wave multi-pulse coupled states even if the efficiency of interaction is rather low due to the factor $\sigma^2\left(\sigma^2+\eta^2\right)^{-1}$.

Stage 2: The localizing pulse is passing in a waveguide.

In this regime the rectangular pulse as the whole is in a waveguide, so $\partial u/\partial x = 0$ exactly and one has to put simply $x = x_0$ in Eqs.(15), (16) in the region $(x_0, L - x_0)$.

Stage3: The localizing pulse is issuing through the facet

$x = L$. This stage is symmetrical to Stage 1, whose solutions, *i.e.* the above-mentioned Eqs.(15), (16), can be inverted and related to the spatial interval of $x \in (L - x_0, L)$.

These solutions include contributions of two types. The first summand in $|C_0|^2$ exhibits a background determined by the mismatch η; the second summand presents the oscillating portion of the solution, *i.e.* the localized part of the pumping light imposed on a background. The generated light contains the only oscillating portion of field that gives the localization condition $x_c^2\left(q_0 q_1 U_0^2 + \eta^2\right) = \pi^2 N^2$, where $N = 0, 1, 2, ...$, so that $x_0 = x_c$ with $N = 1$. The intensity $|C_1|^2$ will be nonzero only in the spatial interval occupied by a slow wave, and therefore, the envelope of the generated

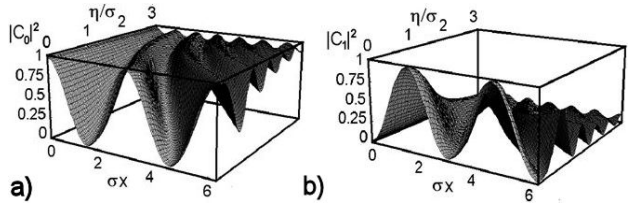

FIGURE 2. Space-frequency distributions for optical components of a two-pulse three-wave coupled state with $q_0 \approx q_1$, $N = 2$, and $Lx = 2\pi$: a) two dark peaks in the zero order of scattering; b) two bright peaks in the first order; this distribution is completely locked with $\eta = 0$.

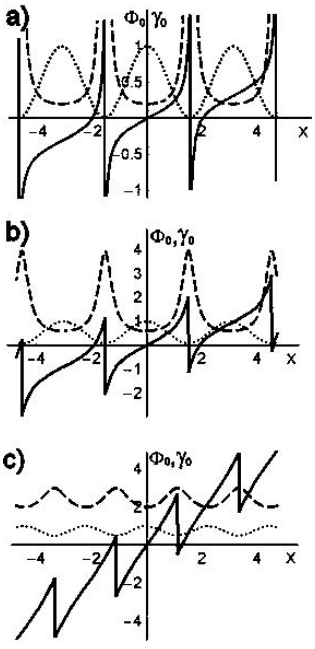

FIGURE 3. Plots for the phase Φ_0 (solid lines) and the frequency γ_0 (dashed lines) in the component C_0 at $\sigma = 0.1$ with: a) $\eta = 0.1$, b) $\eta = 0.3$, and c) $\eta = 1.0$. The intensity distributions $|C_0|^2$ are shown as well by dotted lines.

light wave will be localized, *i.e.* the distribution of $|C_1|^2$ over the transverse extent of non-optical wave has N partial bright peaks in its envelope while the intensity $|C_0|^2$ has N holes (dark peaks). The two-dimensional plots for space-frequency distributions of the optical components in a two-pulse coupled state are shown in Fig.2. Moreover, the obtained solution exhibits the phenomenon of the phase self-modulation in the light wave C_0, because $\gamma_0 = \eta\left(\sigma^2+\eta^2\right)\left\{\eta^2+\sigma^2\cos^2\left[x/\left(\sigma^2+\eta^2\right)\right]\right\}^{-1}$. Plots for the phase Φ_0 and the corresponding frequency γ_0 are shown in Fig.3.

4. Shaping the multi-pulse trains of three-wave weakly coupled states by optical pump and digital modulation of light

Each one-dimensional wave operator in Eqs.(8), (9) is equivalent to the total spatial derivative $\partial/\partial x + c^{-1}\partial/\partial t = d/dx$ taken along the characteristic curve. Thus, $t = t_s + x/c$, where t_s determines the initial instant of time for each of the characteristic curves at the point $x = 0$, and consequently, Eqs.(8), (9) can be rewritten through the total derivatives. Assuming that $C_0(x,t) = C_0(t - x/c)$ and $U(x,t) = u(t - x/v)$, one can integrate the second equation from Eqs.(9) on $x \in [0, L]$ as

$$C_1(L, t_s + L/c) = q_1 C_0(t_s) \times \int_0^L u(t_s + x/c - x/v)\exp(-2i\eta x)\,dx. \quad (17)$$

Here, $u(t) \neq 0$ only with $x \in [0, L]$, and the observation point lies outside the area of interaction. If one takes

$$u = U_0 \sum_{K=0}^{n-1} b_k \{\theta[x - v(t - kT)] - \theta[x - v(t - kT - \tau_0)]\}, \quad (18)$$

$$C_0 = A_0 \sum_{m=0}^{n-1} d_m [\theta(t - t_0 - mT) - \theta(t - t_0 - mT - T)], \quad (19)$$

where n is the number of pulses in these trains, b_k, $d_m \in \{0, 1\}$ and T is the repetition period of the non-optical pulses, whose width $\tau_0 = x_0 v^{-1}$ has to be related to its amplitude U_0, the mismatch η, and the number N from the localization condition, but $\tau_0 \leq T$. The pumping optical pulse train is applied to a waveguide at the instant t_0. Because of $v \ll c$, the spatial size of each optical pulse is much longer than the length of the whole train of non-optical pulses. Once we have decided upon the observation point $x = L$ in such a way that $L = t_0/\left(v^{-1} - c^{-1}\right)$, we obtain that the leading edge of an m-th optical pulse will overtake the leading edge of an m-th non-optical pulse precisely at the point $x = L$. Assuming that the temporal interval $n\tau_0 v c^{-1}$ is negligible, one can put that at each instant of time the whole train of non-optical pulses interacts with a single optical pulse, whose intensity on entering a waveguide is determined by the value of d_m. Let t_0 correspond to the instant of time when the leading edge of the first non-optical pulse, represented by b_0, arrives at the facet $x = L$. Substituting Eqs.(18) and (19) into Eq.(17) and performing the integration, we obtain the amplitude of the generated optical component inherent in an n-pulse train of weakly coupled states, whose partial amplitudes are $g_p = b_p \cap d_p$. Its intensity is given by

$$|C_1|^2 = \frac{q_0}{q_1}\frac{\sigma^2}{\sigma^2+\eta^2}\sum_{p=0}^{n-1} g_p \{\theta[L - v(t - pT)] - \theta[L - v(t - pT + \tau_0)]\} \times \sin^2\left\{\frac{\pi}{\tau_0 v}[L - v(t - pT)]\right\}. \quad (20)$$

The transmitted light intensity can be determined as $|C_0(x)|^2 = |C_0(x=0)|^2 - |C_1(x)|^2$. As a result of the interaction between the incoming optical pulse train and a sequence of non-optical pulses the string of optically pumped three-wave weakly coupled states becomes shaped. In fact, we obtain programmable and electronically controlled switching of the incoming optical pulses that can represent a binary encoded stream of digital data.

5. Selecting the physical mechanism for coupling the light modes

To produce experimentally the above-described non-stationary model of sculpturing collinear three-wave coupled states by the pulsed optical pump, the multi-phonon mechanism of light scattering by a stream of the coherent acoustic phonons, which plays the role of non-optical wave, in a two-mode crystalline waveguide, was chosen. Such a mechanism is based on the photo-elastic effect [9] providing a square-law nonlinearity in an optically anisotropic medium. This effect is partly similar to the Mandelstam-Brillouin scattering of light by heat phonons. There is a good reason to take advantage of the quantum approach to the selected multi-phonon mechanism, which can be considered a sequence of three-particle processes and interpreted as scattering the light quanta, photons, by the quanta of coherent acoustic field, acoustic phonons. When the length of propagation inherent in the coherent acoustic phonons becomes large enough, it is reasonable to believe that acoustic phonons are passing through an infinite medium and, consequently, have well-determined magnitudes of momentum and energy. Under these conditions, each partial act of acousto-optical interaction represents a coherent three-particle process, so that one may use the conservation laws for both the momentum $\vec{p} = \hbar\vec{k}$ and the energy $E = \hbar\omega$, and these laws determine, in fact, the wave vectors $\vec{k}$ and the angular frequencies ω of

the interacting particles. Thus, for instance, the energy conservation laws for each partial three-particle process can be written as $\omega_1 = \omega_0 \pm \Omega$, where ω_0 and ω_1 are the angular frequencies of the incident and scattered photons, respectively; while Ω is the angular frequency of the injected phonons. The plus sign in the energy conservation laws corresponds to originating an anti-Stokes photon, whereas the minus sign meets a Stokes photon. By this is meant that there are two processes, manifesting the annihilation of a phonon (anti-Stokes process) or origination of a Stokes phonon. In the particular case of collinear interaction, the value of Ω can be estimated in terms of the refractive indices n_0 and n_1 for light modes C_0 and C_1, respectively, as

$$\Omega = 2\pi f = \frac{2\pi v}{\lambda} |n_1 - n_0|, \tag{21}$$

where f is now the circular frequency of the coherent acoustic phonons. It is well known from quantum mechanics that the probabilities of annihilating and originating the phonons are proportional to $N_0^{1/2}$ and $(N_0+1)^{1/2}$, respectively, due to the contribution of the spontaneous process in the last case (here N_0 is the number of acoustic phonons per unit volume in a mode). The number N_0 of heat phonons with temperature in a mode is determined in statistical mechanics as

$$N_0 = \left[\exp\left(\frac{\hbar\Omega}{\kappa T}\right) - 1\right]^{-1}, \tag{22}$$

where κ is the Boltzmann constant. Substituting the parameters for ultra-high-frequency acoustic phonons, passing through a crystal at the room temperature, in Eq.(22), we arrive at the inequality

$$N_0 \approx \frac{\kappa T}{\hbar\Omega} \gg 1. \tag{23}$$

This result is true as well for the coherent acoustic phonons injected into a crystal, because an effective temperature inherent in the mode under the excitation of coherent acoustic phonons is much higher than the temperature of a crystal lattice. Thus, at room temperature the contribution of spontaneous processes may be neglected and, consequently, the probabilities of annihilating and originating the acoustic phonons or, what is the same, the probabilities of originating Stokes and anti-Stokes photons are almost equal to each other. By this is meant that both states of polarization are acceptable for the incident light beam applied to the input facet of a waveguide, because they both give practically the same efficiency of collinear acousto-optical interaction.

An upper angular frequency of acoustic phonons in the first Brillouin zone of solid states may be estimated in the approximation of a line lattice as $\Omega_{\max} \approx 2v/\zeta \approx 10^{13}$rad/s (here ζ, is the lattice constant), while in usual practice $\Omega \leq 10^{10}$rad/s. Comparing these estimations even with the lowest photon's angular frequency in visible range, for instance, at the wavelength of λ =671nm, we obtain about $\omega \approx 3\cdot 10^{15}$rad/s and, consequently, $\omega \gg \Omega\max \gg \Omega$. Now it can be seen that, under conventional experimental conditions when the intensities of light and acoustic beams are approximately equal to each other, the number of acoustic phonons is 10^5 times more than the number of photons, so that up to 100% of photons can be scattered due to three-particle processes without any appreciable effect on a stream of acoustic phonons. Consequently, the process of light scattering by coherent acoustic phonons can be considered in approximation of a given phonon field as it was initially assumed in Sec. 2.

6. Estimations and experimental procedure

A schematic arrangement of the performed experiments was similar to the experimental set-up for the filtering technique [10] (see Fig.4). The optical part of our experimental scheme includes two orthogonally oriented polarizer and collinear acousto-optical cells with electronic input via piezoelectric transducer and ultrasound absorber, as depicted in Fig.5. The linearly polarized light pulse is introduced through the input facet of a waveguide and scattered by the acoustic pulse inside a planar crystalline waveguiding structure. As a result, the scattered light beam with an orthogonal state of linear polarization is generated. Then, both these beams are issuing through the output facet of that waveguide. The second polarizer plays a role of the analyzer and makes it possible to select the resulting light modes, as the case requires.

The facets of a crystalline planar structure were inclined with respect to the incoming laser beam to provide the needed reflection of acoustic wave. For this purpose a lithium niobate waveguide of about 30mm in length, oriented along [100]-axis, (synchronism frequency 1.3GHz at λ =0.442nm, temporal aperture 4.6μs, acoustic velocity v=6.57mm/μs [11]) was exploited. We have studied the dynamics of shaping the string of three-wave weakly coupled states by the train of rectangular optical pulses of about 300ns in width each

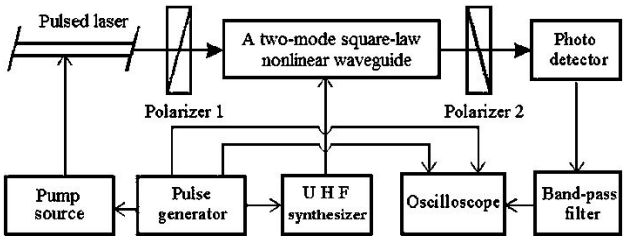

FIGURE 4. General scheme of the experiment with three-wave coupled states.

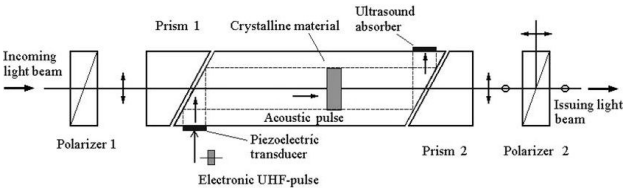

FIGURE 5. Optical scheme of the experiment with three-wave coupled states.

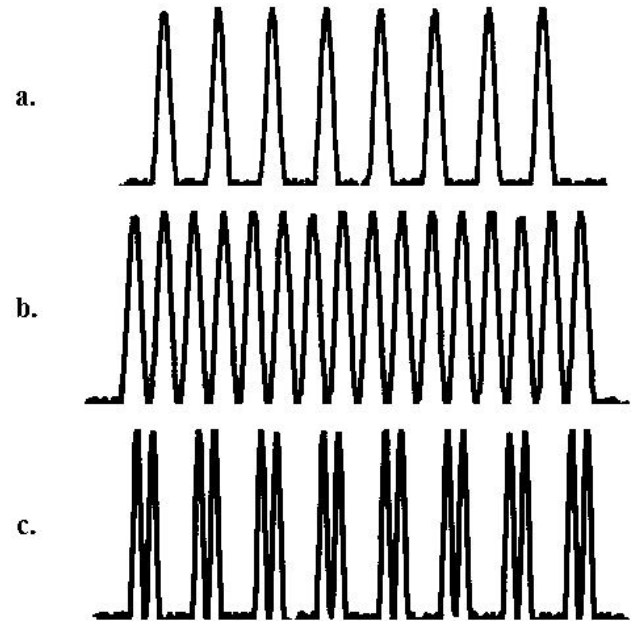

FIGURE 6. Digitized oscilloscope traces for bright optical component $|C_1|^2$ of three-wave coupled state trains with: a) τ_0=τ_c=300ns, Δf=3.15MHz, P=0.5W/mm^2, N=1; b) τ_0=2τ_c=600ns, Δf=3.15MHz, P=0.5W/mm^2, $N=2, N=2$; c) τ_0=τ_c=300ns, Δf=6.31MHz, P=2.0W/mm^2, N=2.

and the train of the localizing rectangular acoustic pulses, whose width τ, power density P, and the frequency mismatch Δf=ηv/π (see Sec. 2) were varied.

To interpret the experimental data, a set of numerical estimations should be taken into account. Let us start from the factor σ, which can be expressed in terms of the values that are usually used during the experiments. This factor is given by [12]

$$\text{a) } \sigma = \frac{\pi}{\lambda}\sqrt{\frac{M_2 P}{2}}, \qquad \text{b) } M_2 = \frac{n_0^3 n_1^3 p^2}{\rho v^3} \tag{24}$$

where p is the acoustic power density, p is an effective photoelastic constant peculiar to the chosen geometry of acousto-optical interaction, and ρ is the crystalline material density. Because with the longitudinal acoustic wave a lithium niobate (LiNbO3) crystalline structure oriented along the [100]-axis with $n_0 = 2.3875$ and $n_1 = 2.2887$ at a wavelength of λ =442nm had been exploited, one has to take $p = p_{41} = -0.151$ and ρ =4.65g/cm^3 (see Ref. 11) providing an acousto-optical figure of merit $M_2 \approx 2.8 \cdot 10^{-18}s^3/g$. To estimate two magnitudes of the factor σ two levels of acoustic power density had been selected, namely, P_1=0.5W/mm^2 and $P2$=0.5W/mm^2. Using Eq.(24a) and the standard ratio 1W/mm$_2$=10^{9}g/s^3, one can obtain $\sigma_1 \approx 0.2$mm^{-1} and $\sigma_2 \approx 0.4$mm^{-1} , respectively. Then, the spatial lengths of acousto-optical coupled states can be estimated for two cases as well. Taking $\tau_1 = 330ns$ and τ_2=660ns, one can find that $x_1 = v\tau_1$=2.17mm and $x_2 = v\tau_2$=4.34mm, respectively. After that, the mismatch parameter η is given by $\eta = \pi\Delta f/v$. Two magnitudes of this parameter can be estimated for a pair of the frequency mismatches, namely, for Δf_1=3MHz and $\Delta f_2 = 6MHz$ as η_1=1.45mm^{-1} and η_2=2.9mm^{-1}, respectively.

Both the efficiency and the intervals of localization are determined by Eq.(6), where one can put $q_0 \approx q_1$. In particular, the efficiency of light scattering is described by the amplitude factor $\sigma^2\left(\sigma^2+\eta^2\right)^{-1}$, while the intervals of shaping the acousto-optical coupled states are dictated by the argument $x\sqrt{\sigma^2+\eta^2}$ under trigonometric sin-function in Eq.(6). Substituting the above-obtained estimations into the last formulas, one can find

$$\begin{aligned} &\text{a) } \frac{\sigma_1^2}{\sigma_1^2+\eta_1^2} = \frac{\sigma_2^2}{\sigma_2^2+\eta_2^2} \approx 0.0186, \\ &\text{b) } x_1\sqrt{\sigma_1^2+\eta_1^2} \approx 3.18 \\ &\text{c) } x_2\sqrt{\sigma_1^2+\eta_1^2} = x_1\sqrt{\sigma_2^2+\eta_2^2} \approx 6.36. \end{aligned} \tag{25}$$

These estimations show that the expected efficiency of localization can reach 1.5 - 2.0 % due to the inequality $\sigma^2 < \eta^2$ and, nevertheless, one can expect shaping in both one- and two-pulse coupled states, because $x_1\sqrt{\sigma_1^2+\eta_1^2} \geq \pi$ and $x_2\sqrt{\sigma_1^2+\eta_1^2} = x_1\sqrt{\sigma_2^2+\eta_2^2} \geq 2\pi$.

The digitized oscilloscope traces for the bright optical component of three-wave coupled states at the waveguide output are shown in Fig. 6. The observed efficiency of localization was about 2%. The trace for the dark optical component $|C_0|^2$ of these coupled states exhibits an analogous train of valleys on a background. Figure 6 shows that with $\tau_0 = \tau_c$=300ns, Δ f=3.15MHz, and P=0.5W/mm^2, one-pulse three-wave acousto-optical coupled states have been observed. Then, with $\tau_0 = 2\tau_c$=600ns, Δ f=3.15MHz, and P=0.5W/mm^2, as well as with $\tau_0 = \tau_c$=300ns, Δ f=6.31MHz, and P=2.0W/mm^2, two-pulse three-wave acousto-optical coupled states have been identified experimentally as well.

7. Conclusion

A distinctive property of the analysis involved is the action of just the pumping light pulses during a three-wave codirectional collinear interaction with the mismatched wave numbers in a two-mode square-law nonlinear waveguide. Theoretical considerations as well as experimental studies of shaping three-wave weakly coupled states have been carried out under these conditions. The analytical model for this process with slightly mismatched wave numbers has been formulated and investigated. The most interesting conclusion from this model is related to the predicate of sculpturing multi-pulse optical components inherent in three-wave coupled states. Both amplitude and phase parameters of their optical components have been estimated theoretically. The developed analysis has been used in an attempt to make the digital modulation of light based on collinear three-wave coupled states potentially acceptable for binary encoded modulation. Using the acousto-optical technique, we have experimentally demonstrated that the trains of collinear three-wave

weakly coupled states can be shaped in a two-mode square-law nonlinear waveguide under pumping from optical pulses.

Acknowledgments

This work was financially supported by the CONACyT, Mexico; projects # U 61237-F and # J 50537-F.

A Biographies

Alexandre S. Shcherbakov received his M.Sc, and Ph.D. in Radio-Physics and Quantum Electronics from Saint-Petersburg State Polytechnic University, Saint Petersburg, Russian Federation in 1972 and 1977, respectively. He joined the staff of this university in 1972, where he was head of the Nonlinear Optics Laboratory, Quantum Electronics Division from 1987 to 2000. From 1980 to 1981 he was with University College London, London, United Kingdom. He has been visiting the National Institute for Astrophysics, Optics, and Electronics, Puebla, Mexico since 2000. For many years, he has focused on the study of nonlinear optical and acousto-optical phenomena as well as optical components inherent in multi-wave solitary waves in crystals, fibers, and semiconductor structures. His interests include processing analog and digital data, high-bit-rate fiber communication, and optical computing.

Arturo Aguirre Lopez received his M.Sc. and Ph.D. in Optics from the National Institute for Astrophysics, Optics and Electronics, Puebla, Mexico, in 2001 and 2005, respectively. His work was related to the investigation of an adaptive photodetector for ultrasonic applications His research includes the study of nonlinear regimes of both collinear and non-collinear acousto-optical interactions, and applying such regimes to digital data processing and optical computing. He is currently working at the Mixteca University of Technology. His research interests include optical information processing and optical computing.

1. N.N. Alhmediev and A. Ankiewicz, *Solitons, Nonlinear Pulses and Beams* (Chapman & Hall, London, 1997).
2. A.S. Shcherbakov, *A Three-Wave Interaction, Stationary Coupled States* (Saint-Petersburg Technical University, St. Petersburg, 1998).
3. Yu.S. Kivshar and G.P. Agrawal, *Optical Solitons: from Fibers to Photonic Crystals* (Academic Press, New-York, 2003).
4. A.P. Sukhorukov, *Nonlinear Wave Interactions in Optics and Radiophysics* (Nauka, Moscow, 1988).
5. R.K. Dodd, J.C. Eilbeck, J.D. Gibbon, and H.C. Morris, *Solitons and Nonlinear Wave Equations* (Academic Press, Orlando, 1984).
6. A.S. Shcherbakov and A. Aguirre Lopez, *Optics Express* **10** (2002) 1398.
7. A.S. Shcherbakov and A. Aguirre Lopez, *Optics Express* **11** (2003) 1643.
8. H.A. Haus, *Waves and Fields in Opto-Electronics* (Prentice Hall, Upper Saddle River NJ, 1984).
9. Yu.I. Sirotin and M.P. Shaskolskaya, *Fundamentals of Crystal Physics* (Mir Publishers, Moscow, 1982).
10. F. Yu, *Introduction to Information Optics* (Academic Press, San Diego, 2001).
11. V.G. Dmitriev, G.G. Gurzadyan, and D.N. Wikogosyan, *Handbook of nonlinear optical crystals*, 3-rd Ed. (Springer-Verlag., New-York, 1999).
12. V.I. Balakshij, V.N. Parygin, and L.E. Chirkov, *Physical Principles of Acousto-Optics* (Radio i Svyaz, Moscow, 1985).